Nitride micro-LEDs and beyond - a decade progress review

H. X. Jiang[*] **and J. Y. Lin**

Department of Electrical and Computer Engineering, Texas Tech University, Lubbock, TX 79409, USA
*hx.jiang@ttu.edu

Abstract: Since their inception, micro-size light emitting diode (μLED) arrays based on III-nitride semiconductors have emerged as a promising technology for a range of applications. This paper provides an overview on a decade progresses on realizing III-nitride μLED based high voltage single-chip AC/DC-LEDs without power converters to address the key compatibility issue between LEDs and AC power grid infrastructure; and high-resolution solid-state self-emissive microdisplays operating in an active driving scheme to address the need of high brightness, efficiency and robustness of microdisplays. These devices utilize the photonic integration approach by integrating μLED arrays on-chip. Other applications of nitride μLED arrays are also discussed.

OCIS codes: (230.0230) Optical devices; (230.3670) Light emitting diodes.

References and links

1. A. Bergh, G. Craford, A. Duggal, and R. Haitz, "The promise and challenge of solid-state lighting," Phys. Today **54**(12), 42 (2001).
2. S. X. Jin, J. Li, J. Z. Li, J. Y. Lin, and H. X. Jiang, "GaN microdisk light emitting diodes," Appl. Phys. Lett. **76**(5), 631 (2000).
3. S. X. Jin, J. Li, J. Z. Li, J. Y. Lin, and H. X. Jiang, "InGaN/GaN quantum well interconnected microdisk light emitting diodes," Appl. Phys. Lett. **77**(20), 3236 (2000).
4. H. X. Jiang, S. X. Jin, J. Li, and J. Y. Lin, "Micro-size LED and detector arrays for mini-displays, hyperbright light emitting diodes, lighting, and UV detector and imaging sensor applications," *US patent 6,410,940*.
5. H. X. Jiang, S. X. Jin, J. Li, J. Shakya, and J. Y. Lin, "III-nitride blue microdisplays," Appl. Phys. Lett. **78**(9), 1303 (2001).
6. H. X. Jiang, J. Y. Lin, and S. X. Jin, "Light emitting diodes for high AC voltage operating and general lighting," US Patents *6,957,899*; *7,210,819*; *7,213,942*.
7. Z. Y. Fan, H. X. Jiang, and J. Y. Lin, "Heterogeneous integrated high voltage DC/AC light emitter," *US Patent 7,221,044*.
8. Z. Y. Fan, H. X. Jiang, and J. Y. Lin, "Micro-LED based high voltage AC/DC indicator lamp," *US Patent 7,535,028*.
9. Z. Y. Fan, "Light emitting diode lamp," *US Patent 7,525,248*.
10. Z. Y. Fan, J. Li, H. X. Jiang, and J. Y. Lin, "AC/DC light emitting diodes with integrated protection mechanism," *US Patent 7,714,348*.
11. Z. Y. Fan, H. X. Jiang, and J. Y. Lin, "Light emitting diode lamp capable of high AC/DC voltage operation," *US Patent 8,272,757*.
12. J. P. Ao, H. Sato, T. Mizobuchi, K. Morioka, S. Kawano, Y. Muramoto, Y. B. Lee, D. Sato, Y. Ohno, and S. Sakai, "Monolithic blue LED series arrays for high-voltage AC operation," Phys. Status Solidi **194**(2), 376–379 (2002).
13. Z. Y. Fan, J. Li, H. X. Jiang, and J. Y. Lin, "Micro-emitter array based full-color micro-display," *US Patent 8,058,663*.
14. J. Day, J. Li, D. Lie, C. Bradford, J. Y. Lin, and H. X. Jiang, "III-Nitride full-scale high-resolution microdisplays," Appl. Phys. Lett. **99**(3), 031116 (2011).
15. J. Y. Lin, J. Day, J. Li, D. Lie, C. Bradford, and H. X. Jiang, "High-resolution group III nitride microdisplays," SPIE Newsroom, December 14 (2011); 10.1117/2.1201112.004001.
16. J. J. D. McKendry, B. R. Rae, Z. Gong, K. R. Muir, B. Guilhabert, D. Massoubre, E. Gu, D. Renshaw, M. D. Dawson, and R. K. Henderson, "Individually addressable AlInGaN micro-LED arrays with CMOS control and subnanosecond output pulses," IEEE Photon. Technol. Lett. **21**(12), 811–813 (2009) (DOI).
17. Y. Narukawa, M. Sano, M. Ichikawa, S. Minato, T. Sakamoto, T. Yamada, and T. Mukai, "Improvement of luminous efficiency in white light emitting diodes by reducing a forward-bias voltage," Jpn. J. Appl. Phys. **46**(40), L963–L965 (2007).

#183172 - $15.00 USD Received 10 Jan 2013; revised 19 Mar 2013; accepted 20 Mar 2013; published 22 Apr 2013

18. H. Yen, W. Y. Yeh, and H. C. Kuo, "GaN alternating current light-emitting device," Phys. Status Solidi **204**(6), 2077–2081 (2007).
19. P. Lamarre, A. Hairston, S. Tobin, K. K. Wong, M. F. Taylor, A. K. Sood, M. B. Reine, M. J. Schurman, I. T. Ferguson, R. Singh, and C. R. Eddy, Jr., "AlGaN p-i-n photodiode arrays for solar-blind applications," Mat. Res. Soc. Symp. **639**, G10.9.1–G10.9.6 (2000).
20. S. Nakamura, S. J. Pearton, and S. N. S. P. Fasol, "G. The blue laser diode: The complete story," Meas. Sci. Technol. **12**(6), 755–756 (2001).
21. D. Vettese, "Microdisplays: Liquid crystal on silicon," Nat. Photonics **4**, 752 (2010).
22. http://www.seoulsemicon.com/en/html/company/press_view.asp?Idx=227.
23. V. Poher, N. Grossman, G. T. Kennedy, K. Nikolic, H. X. Zhang, Z. Gong, E. M. Drakakis, E. Gu, M. D. Dawson, P. M. W. French, P. Degenaar, and M. A. Neil, "Micro-LED arrays: a tool for two-dimensional neuron stimulation," J. Phys. D Appl. Phys. **41**(9), 094014 (2008).
24. N. Grossman, V. Poher, M. S. Grubb, G. T. Kennedy, K. Nikolic, B. McGovern, R. B. Palmini, Z. Gong, E. M. Drakakis, M. A. A. Neil, M. D. Dawson, J. Burrone, and P. Degenaar, "Multi-site optical excitation using ChR2 and micro-LED array," J. Neural Eng. **7**(1), 016004 (2010).
25. P. Degenaar, N. Grossman, M. A. Memon, J. Burrone, M. D. Dawson, E. Drakakis, M. A. Neil, and K. Nikolic, "Optobionic vision--a new genetically enhanced light on retinal prosthesis," J. Neural Eng. **6**(3), 035007 (2009).
26. T. H. Young and C. R. Chen, "Assessment of GaN chips for culturing cerebellar granule neurons," Biomaterials **27**(18), 3361–3367 (2006).
27. M. D. Dawson and M. A. A. Neil, "Micro-pixellated LEDs for science and instrumentation," J. Phys. D Appl. Phys. **41**(9), 090301 (2008).
28. Z. Y. Fan, H. X. Jiang, and J. Y. Lin, "III-nitride micro-emitter arrays: development and applications," J. Phys. D Appl. Phys. **41**(9), 094001 (2008).
29. B. R. Rae, K. R. Muir, Z. Gong, J. McKendry, J. M. Girkin, E. Gu, D. Renshaw, M. D. Dawson, and R. K. Henderson, "A CMOS time-resolved fluorescence lifetime analysis micro-system," Sensors (Basel) **9**(11), 9255–9274 (2009).
30. A. Zarowna-Dabrowska, S. L. Neale, D. Massoubre, J. McKendry, B. R. Rae, R. K. Henderson, M. J. Rose, H. Yin, J. M. Cooper, E. Gu, and M. D. Dawson, "Miniaturized optoelectronic tweezers controlled by GaN micro-pixel light emitting diode arrays," Opt. Express **19**(3), 2720–2728 (2011).
31. K. B. Nam, J. Li, M. L. Nakarmi, J. Y. Lin, and H. X. Jiang, "Unique optical properties of AlGaN alloys and related ultraviolet emitters," Appl. Phys. Lett. **84**(25), 5264 (2004).
32. H. X. Jiang and J. Y. Lin, "III-nitride quantum devices – microphotonics," in *CRC Critical Reviews in Solid State and Materials Sciences*, P. Holloway, Ed., **28**, 131 (2003).
33. V. Adivarahan, S. Wu, W. H. Sun, V. Mandavilli, M. S. Shatalov, G. Simin, J. W. Yang, H. P. Maruska, and M. A. Khan, "High-power deep ultraviolet light-emitting diodes based on a micro-pixel design," Appl. Phys. Lett. **85**(10), 1838 (2004).
34. S. Hwang, M. Islam, B. Zhang, M. Lachab, J. Dion, A. Heidari, H. Nazir, V. Adivarahan, and A. Khan, "A hybrid micro-pixel based deep ultraviolet light-emitting diode lamp," Appl. Phys. Express **4**(1), 012102 (2011).

1. Introduction

Lighting consumes about 20% of total global electricity and produces carbon emission that is roughly 70% of the amount generated by the global automobile flotilla. The most widely used sources of artificial illumination are incandescent lamps, an industry that has not been significantly changed since the 19th century. In recent years, dramatic advances in the development of high brightness light emitting diodes (LEDs) have created the concept of solid-state lighting (SSL) and brought out the potential of replacing incandescent bulbs by LEDs and are rapidly transforming the lighting technology [1]. If used in place of incandescent light bulbs, LED based SSL would provide compactness, longer lifetimes (>20,000 hours for LEDs compared to 2000 hours for incandescent light bulbs), while consuming only a fraction of the electrical power for the same luminous intensity because all of the light produced is used, not wasted in the form of heat, resulting in significant energy and maintenance man-hour savings. Additional benefits include robustness and vibration proof, flexible lighting design, and reduced carbon emission.

All conventional semiconductor LEDs operate under direct current (DC) with typical operating voltages of a few volts (e.g., around 2 volts for red LEDs and around 3.2 volts for blue LEDs). Nonetheless, all the houses and buildings in the world are wired with AC (60 Hz or 50 Hz) 110 volts (or 220 V) power sources. Conventional approaches to use LEDs for lighting include the incorporation of voltage transformer, or combinations of resistors/capacitors in series with LEDs, or Si integrated circuit (IC) based AC/DC power converters, along with electronics controllers and drivers which can be installed separately or built into the LED package. There is also an obvious method for achieving the high voltage

DC/AC operation by wiring together a strand of discrete LEDs. It is evident that these approaches have disadvantages such as added volume, costs, reduced efficiency, increased failure rate and limited current supply. It is recognized by the LED community that fundamental advancements and innovations associated with chip-level integration are the key to bring SSL to reality, analogous to the Si IC technology in revolutionizing the electronics.

Since their inception [2–5], μLED arrays based on III-nitride semiconductors have emerged as a promising technology for various applications. High voltage AC/DC-LEDs were evolved from on-chip integration of μLED arrays and have the potential to fully address the key issue of compatibility of LEDs with AC power grid infrastructure [6–12]. III-nitride based μLED arrays also offer a competing technology for self-emissive microdisplays (μdisplays) [4,5,13–16]. Microdisplays can be used in a variety of devices such as head-wearing displays, head-up displays, camcorders, viewfinders, and pico-projectors and have many commercial and military applications. White LEDs based on III-nitrides have achieved a luminous efficacy of more than 150 lm/W [17], which is much higher than those of other self-emissive devices, such as organic LEDs (OLEDs) and electroluminescent emitters. With the incorporation of multiple quantum wells (MQW) as the active region, LEDs have a narrow emission band of about 25 nm, providing a basis for high color purity and chromatic fidelity. With their intrinsic material properties, LEDs can be operated at extreme conditions such as high or low temperatures (−100° to 120° C) and humidity [14]. All of these intrinsic properties make μLED arrays ideal for μdisplay applications where performance and reliability are critical.

Here, we present an overview on successful examples of Si IC analogy of photonic integrated devices via III-nitride μLED array on-chip integration for emerging technologies: (1) High voltage single-chip AC/DC-LEDs without power conversion to address the key issue of compatibility of LEDs with AC power grid infrastructure [6–12]. (2) High-resolution solid-state self-emissive μdisplays operating in an active driving scheme to address the need of high brightness, efficiency and robustness μdisplays [14,15].

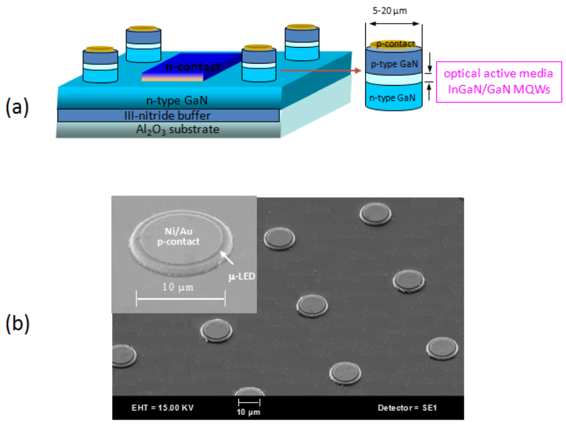

Fig. 1. (a) Schematic layer structure diagram and (b) SEM image of InGaN/GaN quantum well micro-size LEDs (μLEDs) (after Ref. [2]).

#183172 - $15.00 USD Received 10 Jan 2013; revised 19 Mar 2013; accepted 20 Mar 2013; published 22 Apr 2013

2. MicroLED array for high voltage AC/DC-LEDs

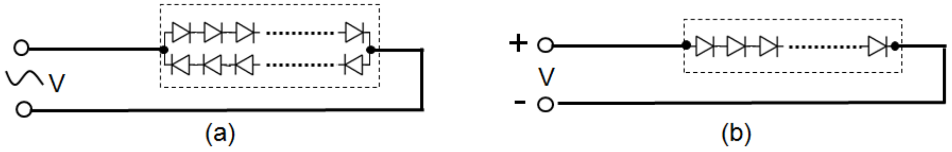

Fig. 2. Schematic conceptual circuit diagrams on how to build a high voltage (a) AC and (b) DC LED device (after Refs. [6] & [7]).

The invention of single-chip high voltage AC/DC-LEDs [6–11] was evolved from the μLED array technology [2–4]. Figure 1 shows an example of a μLED array which consists of plurality of nitride μLEDs fabricated on a single wafer. The insulating nature of sapphire substrate provides an ideal platform for the isolation between individual μLEDs and hence allows serial connection between μLEDs. Figure 2 illustrates the basic principle on how to build single-chip high voltage AC/DC LED devices [6,7]. The number of linked μLEDs is chosen so that the sum of the voltage drop across the individual μLEDs adds up to the voltage of the AC supply. Since LEDs only emit light when they are forward biased, 2 arrays are created for AC operation, one of which lights up during the first half cycle of the AC power source and the other of which lights up when the polarity of the source is reversed, as illustrated in Fig. 2(a). It is obvious that a single array of Fig. 2(b) can operate under a high-voltage DC source, if required.

Figure 3(a) shows the schematic illustration of the layer structure of a single μLED fabricated on sapphire substrate. In order to achieve high voltage operation, a certain number of μLEDs are connected in series - that is the p-contact of one μLED is connected with the n-contact of its neighboring μLED, as illustrated in Fig. 3(b). The serial integration of μLED array on-chip avoids multiple soldering points and thus reduce chip failure rate. Furthermore, with two reverse LED arrays corresponding to the current flow of the positive and negation half cycle of AC voltage, the light on/off frequency is doubled from 50 to 60 Hz VAC frequency to 100-120 Hz, and the effect of light flicking can be minimized. In this μLED integration scheme, a conventional LED is replaced by an array consisting of 40 to 80 μLEDs for 120 VAC for lighting applications. Other design variations such as Wheatstone Bridge type of circuits have also been employed to build monolithic AC-LEDs on single chips [18]. Nevertheless, the fundamental design principle for building high voltage DC/AC LEDs is based on Ohm's law and illustrated in Fig. 2.

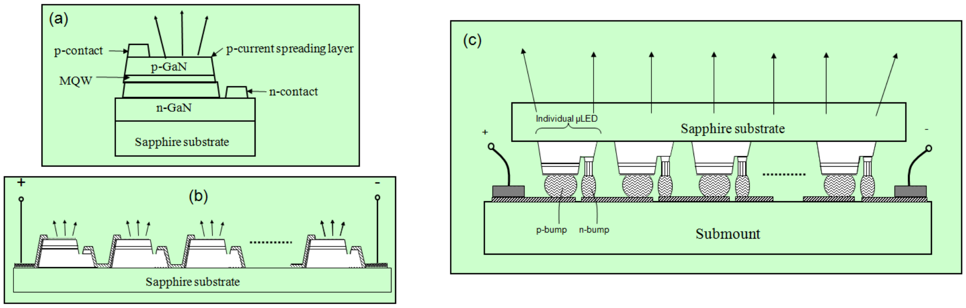

Fig. 3. The cross sectional view of (a) a single low voltage DC LED; (b) high voltage AC/DC LED achieved via monolithic integration of plurality of μLEDs by connecting the p-contact of one μLED to the n-contact of its neighboring μLED; (c) heterogeneous integrated high voltage AC/DC LED achieved via flip-chip bonding with the interconnection between each individual μLED on the submount (after Ref. [7]).

Further improvement to the monolithic integration scheme can be made by heterogeneously integrating μLED array with a passive/active submount through flip-chip bonding [7]. As shown in Fig. 3(b), the submount materials can be chosen so they are electrically insulating and thermally conductive. The submount can be fabricated to contain flip-chip bumps, insulating and metal layers to serially interconnect the μLED array, current limiting resistors and other control and driver circuits. Figure 3(c) shows the cross sectional view of a flip-chip bonded high voltage LED device with the interconnection between each individual μLED on the submount. The final device has two or more outlet connections for the supplied power. Depending on the detailed design, the supplied power may be 12V, 24V, and other DC voltages, or it may be AC voltages such as 110/120V, and 220/240V.

The heterogeneously integrated high voltage DC/AC design shown in Fig. 3(c) provides several improvements comparing with the monolithic integration approach shown in Fig. 3(b). By moving more metal layers from the LED array die to the submount, the LED chip fabrication is easier and the product yield and device reliability will improve. Second improvement is the enhancement of heat dissipation by reducing the thermal resistance. LED performance and lifetime strongly depend on the p-n junction temperature. Furthermore, with flip-chip bonding, now the light is extracted from the transparent substrate side. In the design shown in Fig. 3(b), light is extracted from the nitride device side. The n-contact, p-contact, current spreading layer, and interconnection layer, will partially block or absorb the light extraction. For the heterogeneous integration design in Fig. 3(c), since there are no metal contacts or layers on the substrate side, light absorption is avoided, and the light efficiency is increased.

For III-nitride LED wafers grown on the sapphire substrates, AC-LEDs are fully compatible with the traditional DC LED production lines. Both the conventional DC-LEDs and AC-LEDs have the n- and p-contacts fabricated on the same side of the LED wafer due to the electrically insulating nature of sapphire substrate and require plasma dry etching to etch into n-GaN to form the LED mesa. The sapphire substrate provides a natural base for the isolation of individual μLEDs. Therefore, the chip cost for both AC-LED and DC-LED is very similar. However, the major cost saving for AC-LEDs will be in the packaging because of the elimination of transformers and other electronics drivers. On the other hand, to fabricate AC-LEDs from LED structures grown on conductive SiC or Si substrates, the isolation between μLEDs can be achieved by incorporating a layer of insulating material between the substrate and LED layer structure [9]. This may require modification to the existing LED layer structures. For InGaN LEDs, AlN buffer/template layer has been demonstrated to be an excellent alternative to GaN buffer/template layer and the highly insulating AlN can provide an ideal solution for μLEDs isolation for LED structures grown on conductive SiC or Si substrates.

For lighting applications, the typical LED chip size is 1 mm x 1 mm or greater (named power LEDs). Each mini-LEDs within the power AC-LED array has a similar chip size as the traditional indicator DC-LEDs and experiences the same operating voltage and current density as the traditional DC-LEDs. However, because AC-LEDs are effectively operating under a pulsed mode (60 Hz) and are in the "on" state only for a half of the cycle, it is expected that AC-LEDs can be designed to handle higher current density than the traditional DC-LEDs.

#183172 - $15.00 USD Received 10 Jan 2013; revised 19 Mar 2013; accepted 20 Mar 2013; published 22 Apr 2013

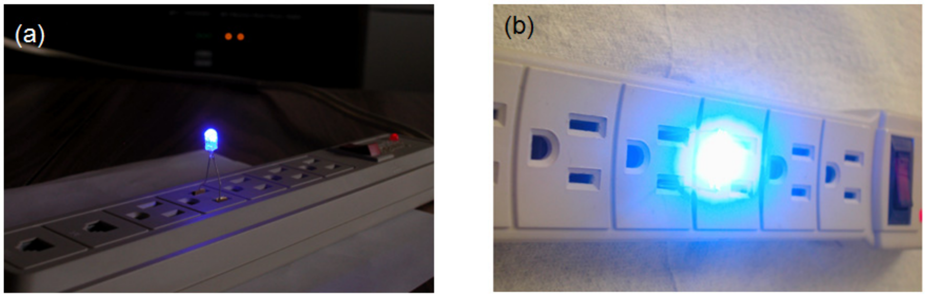

Fig. 4. Photos of one of our (a) high voltage indicator AC-LEDs with chip size of about 0.3 mm x 0.3 mm and (b) high voltage power AC-LEDs with chip size of about 1 mm x 1mm directly plugged in the 120 VAC power outlets without power converters.

Another huge advantage of the integration approach for obtaining high voltage AC/DC LEDs is the flexibility of incorporating a protection mechanism on the chip level by limiting the influence of the line voltage variation on the current [10]. The protection element can be directly integrated on the AC/DC LED chip or it may be integrated on the submount of the flip-chip bonded AC/DC LED device and has the function of reduce or ease the influence of voltage variation on AC/DC LED device performance and lifetime. It is very interesting to realize that a current-limiting resistor can be monolithically integrated on the same AC/DC LED chip and fabricated from the same LED wafer [10].

We have fabricated both high voltage power AC-LEDs (with chip size of about 1 mm x 1 mm) and indicator AC-LEDs (with chip size of about 0.3 mm x 0.3 mm). Figure 4 are the photos of packaged (a) 5 mm indicator AC-LED lamp and (b) power AC-LED directly plugged in the 120 VAC power outlets without power converters. The AC indicator LED lamps are very suitable for uses in indication, signage, night lamps and holiday decorative tree lighting [8]. Since each LED lamp runs with a current of no more than 0.5 mA, there is almost no limitation on the number of AC-LED lamps connected in the tree lighting string, and the LED string can be directly plugged into the house-hold AC power supply without transformer or rectifier. A power AC-LED lamp runs under a 120/220 VAC with a current around 20 mA to achieve a high brightness level for general lighting application. One can further integrate plurality of high voltage AC/DC-LED chips on a submount to form a compact AC/DC-LED lamp for ultra-high brightness applications [11].

It is very interesting to note that compared to DC-LEDs, no optical power is lost during the AC cycle for AC-LEDs. The effective optical output power of an LED under AC operation is the integrated power over a half-period in a 60 Hz cycle, which can be evaluated according to

$$P_{ave} = \frac{1}{\pi}\int_0^{\pi} P(t)dt, \qquad (1)$$

where the LED optical power is written in terms the forward voltage (*V)* and current *(I)* according to the diode equation,

$$P_{output} = CI_0(e^{\frac{q(V-IR)}{nkT}} - 1), \qquad (2)$$

and the voltage produced by an AC power supply is sinusoidal, $V = V_o \sin 2\pi ft = V_o \sin \omega t$, with the root-mean-square voltage being $V_{rms} = 0.707V_0$. In our single-chip AC-LED design shown in Figs. 2 and 3, V_{rms} is divided among *n* mini-LEDs, so V_{rms} across each mini-LED will be about the same as a traditional DC-LED. By evaluating the above integral, it can be shown that the effective (or average) optical power output of an LED under AC operation is comparable to the output power under DC operation. This is due to the fact that the diode behavior (turn-on behavior) is embedded in the responses.

3. MicroLED based full scale high-resolution microdisplays

To achieve a high-information-content μdisplays that are capable of delivering video graphics images, the desired driving approach is active matrix driving. The challenge for achieving μLED based μdisplay with active driving is that III-nitride μLEDs cannot be fabricated directly over Si IC circuitry. To overcome the above difficulty, we have adopted the hybrid μdisplay concept. An energy efficient active driving scheme is accomplished by integrating μLED arrays with CMOS active matrix drivers that are flip-chip bonded together via indium metal bumps [14]. CMOS active matrix 640 x 480 and 160 x120 microdisplay controller ICs with μLED current of 0.5μA to 10μA have been designed and fabricated in a CMOS process [14]. The flip-chip bonding of μLED arrays with CMOS active matrix drivers is an extension of flip-chip bonding of focal plane detector array with CMOS read-out-circuitry, which is a highly mature and widely deployed technology [19].

Figure 5(a) shows a schematic illustration of the μdisplay which consists of plurality of InGaN μLEDs as pixels arranged into matrix format on a sapphire substrate and the μLED array is heterogeneously integrated onto a Si CMOS IC driver chip using indium bump bonding. The polished back surface of the transparent sapphire substrate is used to display images. The pixels share a common anode (n-type contact) with independently controllable cathode (p-type contact). Compared to the earlier version of a passive driving InGaN μdisplay [5], the hybrid integration of the InGaN μdisplay die with the Si CMOS driving circuit IC chip die means that hundreds or thousands of the signal connections between the μdisplay and the driving circuit have been accomplished in a single flip-chip bonding package through the indium metal bumps [14]. This active matrix display also means that each pixel is geared with its own pixel driver circuit in CMOS that is capable of storing data and driving each individual μLED. The interface requirements of this hybridized package are thereby reduced to the few lines required for the signal and power connections.

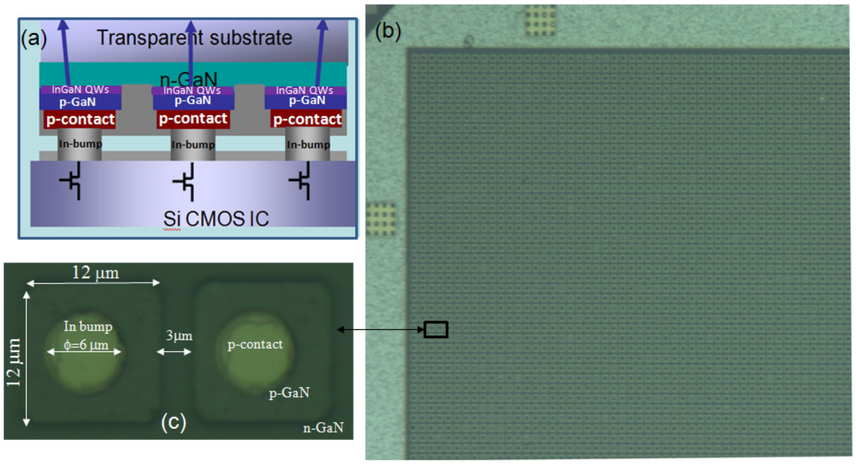

Fig. 5. (a) Illustration of flip-chip bonding between μLED matrix array and CMOS driver IC via indium bumps to form a highly integrated microdisplay in one package. (b) Optical microscopy image of a full scale (640 x 480 pixels) InGaN μLED array. (c) The zoom-in image of a flip-chip bonded package with μLED pixels and indium bumps viewed from the transparent sapphire side (after Ref. [14]).

The optical image of a segment of an individually diced μLED array chip is shown in Fig. 5(b), which illustrates more details of the fabricated devices. Micro-LED pixels and indium metal bumps fabricated by thermal evaporation on the μLED pixels seen from the transparent sapphire side shown Fig. 5(c) demonstrated the realization of ~6 μm indium bumps with excellent size uniformity. Figure 6(a) shows a fully assembled InGaN μdisplay. Figure 6(b) shows a grayscale projected image of a leopard from a green InGaN VGA microdisplay (640 x 480 pixels) and reveals that the fabricated μdisplays are capable of delivering real time video graphics images.

To obtain a sense of the microdisplay brightness, the luminance of the green μLED pixels has been measured. As shown in Fig. 6(c), a 12 μm pixel outputs roughly 1 mcd/μA and the luminance increases almost linearly with driving current (*I*) for $I < 100$ μA. For a μdisplay with a pitch distance of 15 μm, when every pixel within the array is lit up and operates at 1 μA, the brightness of the μdisplay can be calculated to be ~4x10^6 cd/m^2. This luminance level is several orders of magnitude higher than those of LCD and OLEDs. Based on the pixel I-V characteristics in Fig. 6(d), at $I = 1$ μA, a green μLED pixel has an operating voltage of around 2.6 V. This means that the power dissipation within the μLED array is only about 0.8 W for a full VGA (640 x 480 pixels) μdisplay if every pixel within the μLED array is lit up simultaneously. This estimate represents the upper limit of power dissipation since normally only a fraction (~25%) of pixels are lit up for graphical video image displays.

Notice also that 1 μA driving current translates to a current density of about 0.7 A/cm^2 for a 12 μm pixel, which is about 1/30 of the typical value (22 A/cm^2) in conventional DC indicator LEDs having an average chip size of 0.3 mm x 0.3 μm and normally operating under 20 mA. The expected lifetime of DC indicator LEDs exceeds 100,000 hours under normal operating conditions (i.e., $I = 20$ mA). These estimates also imply that the lifetime of III-nitride μLED array should be as long as those of indicator LEDs.

Another outstanding feature of InGaN based self-emissive μdisplays is their ability to operate under harsh conditions and at high or low temperatures. The operating temperature (*T*) dependence of the optical output power of our μLEDs has been measured. The intensity of the μLED emission decreased by about 10% when *T* was raised from room temperature to + 100 °C and remained almost constant when *T* was cooled down from room temperature to −100 °C, while the operating voltage at 0.1 mA decreased from 4.1 V at −100 °C to 2.9 V at + 100 °C. This continuous reduction in the operating voltage with increasing *T* is due to thermal activation of free holes (*p*) described by the process of $p \sim \exp(-E_A/kT)$, where the Mg acceptor activation energy (E_A) in GaN is about 160 meV [20]. The outstanding thermal stability is a direct attribute of III-nitride semiconductors.

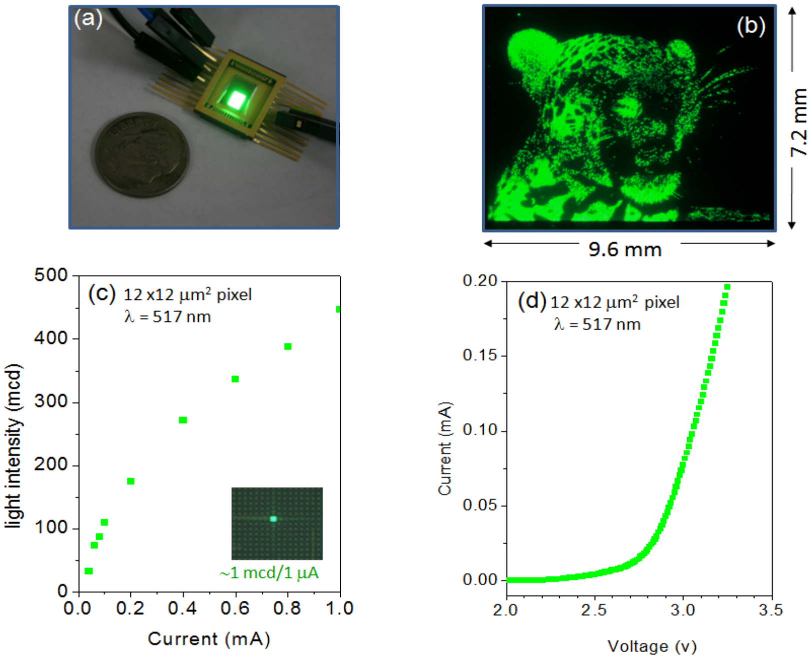

Fig. 6. Demonstration of an III-nitride self-emissive µdisplay. (a) A fully assembled InGaN µdisplay operating at a driving current of about 1 µA per pixel. (b) A grayscale projected image of a leopard from a green VGA InGaN microdisplay (having 640 x 480 pixel with a pixel size of 12 µm and a pitch distance of 15 µm) operating at a driving current of 1 µA per pixel. (c) L-I characteristic of a green µLED pixel. (d) I-V characteristic of a green µLED pixel (after Ref. 14).

Unique features of III-nitride µdisplays are summarized in Table 1. Compared with other technologies, III-nitride µdisplays can potentially provide superior performance. Unlike liquid crystal displays (LCDs) that normally require an external light source [21], III-nitride µdisplays are self-emissive and result in both space and power saving and allow viewing from any angle without color shift and degradation in contrast. LCDs also require the use of heaters when operating in low temperature environments. The luminance level of III-nitride µdisplays is several orders of magnitude higher than those of LCD and OLEDs. OLEDs must be driven at current densities many orders of magnitude lower than semiconductor LEDs to obtain devices with a reasonable lifetime and hence are not suitable for high-intensity use. Digital light processing (DLP) and laser beam steering (LBS) devices require the use of rapidly scanning microelectromechanical (MEMS) mirrors and separate light sources such as LEDs or laser diodes (LDs), which adds complexity, volume, and cost to the devices. Furthermore, the service lifetimes of MEMS and LDs are shorter than LEDs. We believe that the remaining future challenge of III-nitride µdisplays is to achieve full color µdisplays based on monolithic vertically stacked red-green-blue (RGB) pixels [13]. Currently, it is highly challenging to obtain InGaN LED wafers with red color emission. This problem originates from the basic material issues concerning InGaN alloys with relatively high In-contents, which is expected to be overcome with further research.

Table 1. Feature of III-nitride µLED based µ displays (after Ref. [14])

Mechanism	**Luminous efficacy**	**Luminance**	**Contrast ratio**	**Response time**	**Operating temperature**	**Shock Resistance**	**Lifetime/cost**
Self-emissive	High	~10^5 cd/m^2 (full color) ~10^7cd/m^2 (blue/green)	Very high >10,000:1	ns	−100 to 120°C	High	Long/Low

#183172 - $15.00 USD Received 10 Jan 2013; revised 19 Mar 2013; accepted 20 Mar 2013; published 22 Apr 2013

4. Summary

The development of III-nitride μLEDs has enabled the realization of several novel photonic devices. The serial integration of μLED arrays on chip has led to the invention of single chip high voltage AC/DC-LEDs [6–11]. So far, power AC/DC-LEDs based on monolithic integration approach have reached high performance level and are currently commercially available [22]. The technology not only directly address the key compatibility issue between LEDs and AC power grid infrastructure for lighting, but also provide DC LEDs operating under varying high voltages for various applications including automobile headlights at reduced cost and increased reliability. The concept of an integrated single-chip LED device operating under high AC/DC voltages is expected to unfold a new paradigm for SSL.

The first μdisplay based on inorganic semiconductors capable of delivering real time video graphics images has been demonstrated [14]. This high-resolution solid-state self-emissive μdisplay operating in an active driving scheme was achieved via integration of III-nitride μLED arrays with Si CMOS driving IC chips. Microdisplays can be used in a variety of devices such as head-wearing displays, head-up displays, camcorders, viewfinders, and pico-projectors. In many cases, μdisplays may need to operate under sun light. Both LCD and OLED based μdisplays may not be bright enough to carry out the necessary functions, whereas III-nitride μLED based μdisplays could offer a solution. Due to the high brightness together with other unique features, III-nitride μdisplays appear to be a promising competing technology for handheld/mobile pico-projectors.

III-nitride μLED arrays with emission wavelength from visible to ultraviolet range are ideal light sources for optogenetic neuromodulation [23–26] and have provided a new avenue for the multi-site photostimulation of neuron cells and offers the opportunity to probe biological neuron networks at the network level [24,25]. These devices are expected to continue to find other applications such as in microarray biosensors based on fluorescence excitation and detection [26–29], miniaturized optoelectronic tweezers [30], etc.

Another application of III-nitride μLED array is to improve LED's light extraction efficiency and current spreading [3,4]. Most light generated in LEDs tends to be trapped in the semiconductor by total internal reflection. Consequently, the high refractive index (*n*) limits the photon extraction efficiency of conventional planar GaN LEDs to less than 5%. It was shown that for interconnected μLEDs, the overall emission efficiency was increased over the conventional LEDs for the same device area [3]. The exclusive features of interconnected μLEDs are particularly beneficial to UV emitters as the light extraction becomes even more difficult in UV wavelengths due to the incorporation of Al. It is known that in UV LEDs using c-plane Al-rich $Al_xGa_{1-x}N$ as active layers, the most dominant emission will be polarized along the c-axis, which implies that UV photons can no longer be easily extracted from the surface [31]. Our measurements showed that for 340 nm UV LEDs the interconnected μLED architecture provides reduced operating voltage and enhanced power output due to improved extraction efficiency and current spreading [32]. At 20 mA, the enhancement is almost 100% [32]. The μLED array architecture is also highly effective for improving the overall efficiency of deep UV LEDs [33,34].

Acknowledgment

Our research program at Texas Tech University is supported by grants from NSF, DOE, DARPA/AFOSR, DHS, and ARO/JTO. The development efforts of μLED array based high voltage AC/DC LEDs and μdisplays were supported by SBIR grants from ONR, NSF, and US Army (Night Vision and Electronic Sensors Directorate). This invited review represents a short summary of a decade progress made by our group and we are indebted to our program managers as well as to our current and former collaborators and group members for their persistent support. We are also grateful to the AT&T foundation for the support of Ed Whitacre and Linda Whitacre endowed chairs.